Fiber optic gyro for space applications. Results of R&D and flight tests

Yu.N.Korkishko, V.A.Fedorov, V.E.Prilutskiy,
V.G.Ponomarev, I.V.Morev, D.V.Obuhovich, S.M.
Kostritskii, A.I.Zuev, V.K.Varnakov, A.V.Belashenko
Optolink RPC LLC,
Moscow, Russia
opto@optolink.ru

E.N.Yakimov, G.V.Titov, A.V.Ovchinnikov,
I.B.Abdul'minov, S.V.Latyntsev
JSC "Academician M.F.Reshetnev Information
Satellite Systems",
Zheleznogorsk, Krasnoyarsk region, Russia

Abstract— **The aims of the current work are the research and development and flight tests of fiber-optic gyro for space applications VOBIS. Space-grade FOGs VOBIS are developed for the tasks of spacecraft orientation and navigation at the high orbit and are long-life radiation resistant. Its' estimated operation time is 15 years in high vacuum and radiation environment.**

Keywords—fiber optical gyroscope, space application

I. INTRODUCTION

At present time fiber-optic gyroscopes (FOGs) with closed-loop feedback scheme of operation are becoming widely used in inertial navigation complexes. In FOGs with closed-loop scheme the feedback mechanism keeps the zero signal level by compensating the Sagnac phase shift with additional phase counter-shift. The value of the phase counter-shift allows one to obtain information about the angular rate of the device rotation [1].

Space satellites operate at high altitudes of 200-80000 km and carry out missions in the general areas of earth and space science, technology demonstration, remote sensing, commercial telecommunication and national defense. The mission of the satellite dictates the choice of the orbital path which may take it through Van Allen radiation belt and always radiated by cosmic rays.

The aims of the current work are the research and development and flight tests of fiber-optic gyro for space applications VOBIS. Space-grade FOGs VOBIS are developed for the tasks of sattellite orientation and navigation at any orbit (flight tests performed in Geostationery orbit (GEO)) and are long-life radiation resistant. Its' estimated operation time is 15 years in high vacuum and radiation environment.

II. FOG VOBIS CONFIGURATION

A. Configuration

Device itself is a monoblock consisting of three autonomous orthogonally placed fiber-optic gyros, and is used for the tasks of space vehicle orientation and navigation at any orbit during its estimated operation time of 15 years in high vacuum and radiation environment.

Angular rate measurement channels are independent so that a channel failure does not affect the other operational measurement channels by design.

Each optical measurement channel consists of a light source (superlumenescent diode (SLD)) with optical fiber output from radiation-resistant single mode polarization-maintaining fiber, photodiode (PD) with optical fiber input from radiation-resistant multi-mode isotropic fiber, polariser-splitter (PS) on a $LiNbO_3$ chip with inputs and outputs made from radiation-resistant single mode polarization-maintaining fiber and a ring interferometer, sensitive to the angular rate of rotation (Fig.1). Blocks of electronics maintaining several functions such as power supply of FOG elements, photodiode signal processing and phase modulators control, are separated from the optical scheme. The measured angular rate data is output in the format of binary phase-manipulated code.

Thermal exchange of the device is performed through the base surface of mounting, the unit is qualified in temperature range -30 ^{0}C to +40 ^{0}C.

The ring interferometer consists of a multifunctional integrated-optic chip (MIOC) performed on the substrate of $LiNbO_3$, and of radiation-resistant polarization-maintaining optical fiber loop (FL). All elements of optical scheme with the exception of SLD and PD are serially produces by RPC "Optolink".
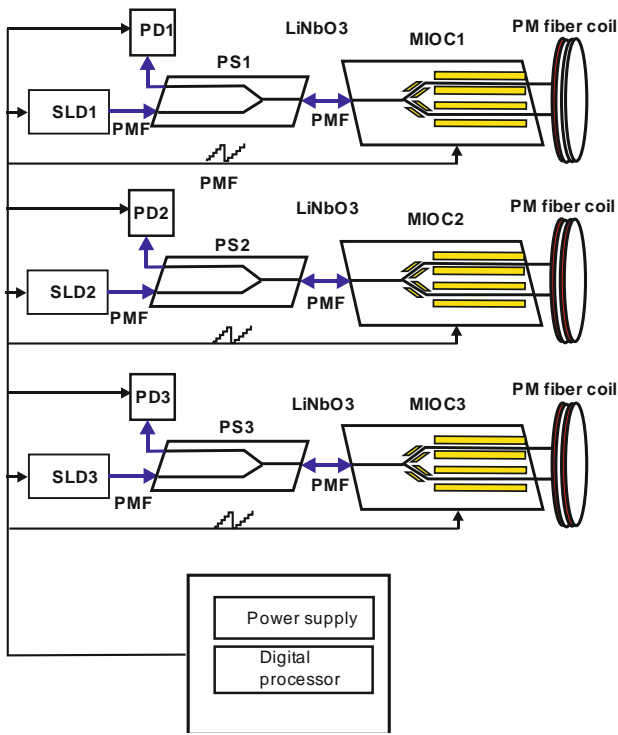
Fig. 1. Configuration of FOG VOBIS.

B. Commercial Off The Shelf (COTS) components

We tried to minimize the number of purchased optical components in our FOG. VOBIS is comprising some of optical devices: active optoelectronic components (SLED, Receiver and MIOC), passive optical component (Polarising Splitter) and fiber coil for the Sagnac interferometer). As no space qualified alternative were available on the market, these optical devices were to be procured on commercial standard (Commercial Off The Shelf or COTS components) and upgraded to space standard. Fortunately, the main components (MIOC, PS, fiber coil and partially Receiver) are produced by Optolink. The SLED's used are taken from the Telecom Industry, and some qualification data (such as Telcordia qualification) were already available. The objective is then to procure a batch of components and to qualify this batch with a representative sample. The qualification of the technology has been achieved in three steps: component procurement, qualification plan definition; qualification testing.

C. Radiation hard polarization maintaining fiber (PMF)

We have developed a technology for forming fluorine-doped silica glass light-reflecting cladding with $\Delta n \sim -(8.5 - 9.5) \times 10^{-3}$ using SiF_4 as fluorine-agent. After fluorine-doped silica glass cladding deposition finish inside supporting tube deposits SiO_2 layers that form fiber core by $SiCl_4$ oxidation.

Optical fibers have been drawn out on drawing tower using a high-temperature graphite heater with simultaneous covering with protecting and strengthening two-layer UV-curable acrylo-urethane coating. Silica fiber diameter is $80\pm1,5\mu m$.

Mode field diameter measured upon TIA standard equals $9.2\pm0.2\mu m$ at $\lambda=1.55\mu m$. The refractive index profile is shown at Fig.2.
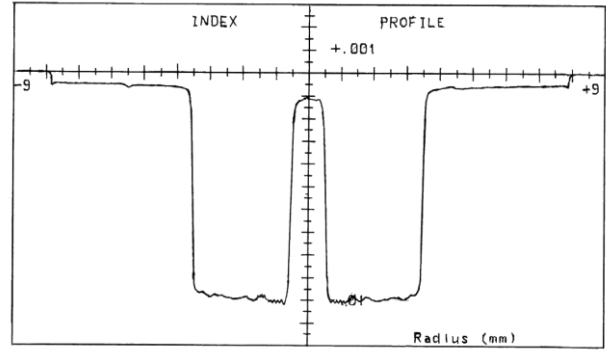

Fig. 2. The refractive index profile of radiation hard polarization maintaining fiber.

Quadrupole winding technique implies winding a coil from a single segment of fiber, starting at the center of the segment, winding outward toward the ends, alternately from one or another of two supply spools, in a geometrically structured way. Indeed, optical fiber is elastic but very delicate. Elasticity implies a need to keep fiber always under constant tension during winding. Delicacy implies a need to control not only in-process fiber tension, but also fiber flexure or curvature, and a surface contact. The coil is placed at temperature isolated plate with diameter of 100 mm. Our fiber coil winding machine was specially developed basing on standard wire winding machine.

D. Integrated optical components

One of the main fiber optical gyroscope's components is a multifunctional integrated optical chip (MIOC). Optolink's MIOC is a solid state waveguide device on X-cut $LiNbO_3$ substrate fabricated by High-Temperature Proton Exchange method (HTPE) [2]. It includes a linear polarizer, Y-junction coupler and two pairs of electro-optic phase modulators. Light coming from the optical fiber coupler is linearly polarized within the MIOC to greater than 60 dB polarisation. This high degree of polarization minimizes bias uncertainty due to polarization non-reciprocity. The Y-junction coupler within the MIOC splits the light into equal amplitude waves, each directed along a separate waveguide within the MIOC. Each of the resulting waves pass through an electrooptical phase modulator and after two waves counterpropagate around the optical PM optical fiber sensor coil.

A very important advantage of proton exchange (PE) waveguides is following. In such waveguides the extraordinary refraction index is increasing, while refraction index of ordinary ray is decreasing. As a result, proton exchanged waveguides support propagation only extraordinary polarization modes (TE in our case). Therefore, it is no necessity to use in the fiber optical gyroscope a polarizer, which brings additional loss.

38

It is well known, that standard technology of PE waveguide (APE-technology) [3] applies a two-level process, which consists of a PE, (melting pure or diluted by lithium benzoate benzoic acid as a rule) and subsequent annealing (Fig.4a). It was recently obtained, that different defects are formed in the surface area of waveguide due to different phase transitions [4]. These defects are sources of additional scattering of light.

In paper [2] we reported the fabrication and characterization of $LiNbO_3$ optical waveguides prepared by HTPE process. HTPE process, in contrast to APE, is a one step process and does not allow any phase transitions (Fig.3), and, therefore, allows one to achieve the smaller optical losses and higher electro-optical coefficients.
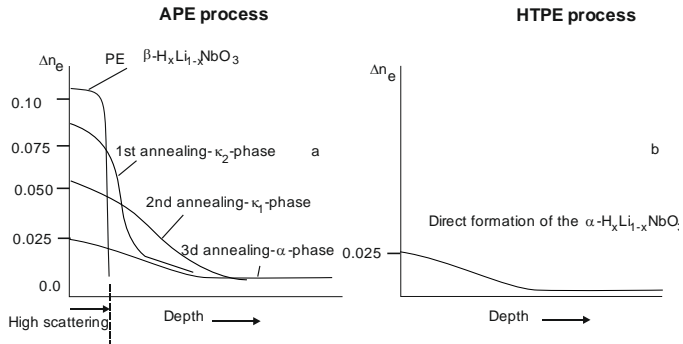

Fig. 3. Formation of α-phase PE $LiNbO_3$ waveguides by APE (a) and HTPE (b) processes.

The HTPE processes are held in the specially developed containers. The specially developed metals and dielectric films used as masks to provide locality proton exchange diffusion. Then by vacuum deposition of electrodes, the integrated electro-optical phase modulators are formed on both arms of Y-splitter. Then the end surfaces are cut (the angle is 10 degree to the Y axis), polished, and finally coupled with PM fiber pigtails. The final steps are packaging and welding electrodes.

The PS is fabricated by same technology as MIOC and is packaged at same monoblock as MIOC. It includes a linear polarizer and an Y-junction coupler.

III. ELECTRONICS

Digital signal processor (DSP) generates voltage for "sawtooth" light modulation for compensation of Sagnac phase shift and to make fixed phase shift of $\pi/2$. As a result, each channel is working in closed-loop regime. Fig.4 shows the scheme of DSP.

Analog signal from the phase sensitive detector (PSD) that processes the output of the FOG photodetector is amplified and passed to high frequency analog to digital converter (ADC). The digital signal is demodulated by Altera Field Programmable Gate Array (FPGA). Obtained code passed to digital integrator. The code of signal from integrator is using

to obtain the slop of phase "saw-tooth" which corresponds to rotation rate. The Digital to Analog converter creates the analog signal as saw-tooth voltage and pass it to MIOC. The wideband integrated optic phase modulators placed at both arms of MIOC are employed to introduce phase ramp modulation, thus enabling close-loop operation. The loop closure scheme uses a digitally synthesized saw-tooth (serrodyne modulation) of 2π amplitude in optical phase shift. In this case the Sagnac phase shift is compensated by saw-tooth modulation of light with calibrated amplitude 2π and frequency f, determined from well-known equation:

$$f = \frac{D}{n\lambda}\,\Omega$$

where Ω is a rotation rate, D – diameter of fiber coil, n-effective refractive index of waveguiding mode, λ - wavelength.

The frequency of resulting ramp is then a digital measure of the rotation rate, with each ramp reset proportional to the angular turned, i.e. one ramp is equal to $\frac{n\lambda}{D}$. To increase resolution of gyro the rotation rate is determined by measuring slop of phase saw-tooth.
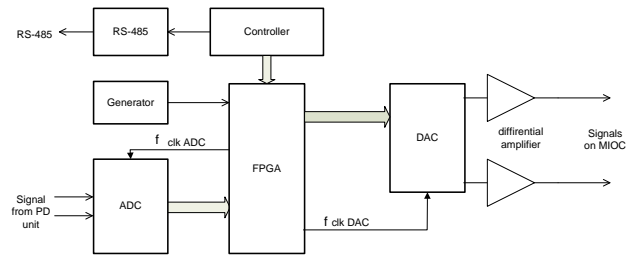

Fig. 4. Block diagram of DSP. ADC – analog digital converter, DAC – digital analog converter, FPGA – Field Programmable Gate Array, PD unit – photodetector unit.

DSP represents the circuit based on Altera's FPGA. DSP is connected with high-speed ADC and with two fast Analog Devices's DAC. Clock pulse for DAC and ADC are drawing up by FPGA. Work of FPGA are clocked by external thermo-stabilized generator.

On one of DSP the Atmel's microcontroller is established which is working as the loader for FPGA. Controller provides an exchange on interface MIL STD 1553 with external devices. The monitor for device settings is realized based on this controller. Except for loading FPGA, the controller reads out the data of measurements from FPGA.

The shaper of clock pulses transforms clock frequency to a set of impulses for synchronous work management of all devices and units. Clock frequency f_{clk} gets out to multiple frequency AM f_{am} Clock pulses for DAC are formed on fronts AM. Clock pulses for ADC are formed so that to exclude measurements on fronts of a signal from PD.

The circuit of processing the signal coming from PD consists of the integration block, the buffer for storage of the measured value and the differencing circuit. The sum of the

values of mismatch signal measured on the current phase AM is collected at integration block. On the buffer the sum of the values measured on previous phase AM is stored. After the measurements the values from the integration block and from the buffer pass to the differencing circuit. Depending on current phase of AM, one number passes as deducted and another as the subtractor. Thus the amplitude of a variable signal is allocated taking into account its sign.

The code with sign, corresponding to a sign of a mismatch signal, passes to the digital integrator which consists of the multiplier and the summing unit with the circuit of restriction. The time constant of the digital integrator is setting by the multiplier. The summing unit is used as the integrator. The code from the integrator passes to the shaper of the code for compensating modulation and through the digital filter to the serial interface of connection with the controller.

The shaper of a code for compensating modulation includes the summing unit which forms the "saw-tooth" code and the second summing unit which is used in a contour of a digital regulator of amplitude of compensating modulation. The signal from the circuit of processing of a signal from PD taken off at the moment of recessions of "saw-tooth" serves as signal of a mismatch for a digital regulator of amplitude of compensating modulation. The same signal is used for fine tuning of amplitude of auxiliary modulation.

There are two main sources of scale factor errors: (i) the finite flyback time and (ii) the nonstability of phase amplitude. To avoid influence of first factor we used the special transformation in the circuit, which creates a control voltage signal for MIOC. In our scheme the flyback time excludes from transmission characteristics of electro-optical modulator. The nonstability of phase amplitude is minimized by creating the astatic follow-up system. The response of device on periodic signal with calibrated constant period is considered as an error signal. Special circuit, independently on FOG moving, generates this periodic signal securing the zero error of stabilization of phase saw-tooth at 2π value at stationary rate and negligibly small error of this value at dynamic rate.

IV. FOG VOBIS PERFORMANCE

In our design we reduce as much as possible the fundamental limitation of IFOG performance:

Optical losses

Sensitivity of FOG is limited by shot noise that goes as the square root of the power that decreases with fiber length. However, the Sagnac effect increases with the length of the fiber. These two competing effects set the length of the fiber for a given sensitivity.

Thermal Noise

Time dependent temperature gradient along the length of the fiber can introduce spurious phase shifts due to the temperature dependence of the refractive index of fiber. To minimize this effect the fibers with smaller dn/dT dependence should be used. Also, quadropole winding such that equidistant points from fiber center are physically close to each other strongly reduce this effect.

Backscattering of light

Backscatter at the output-input couplers and MIOC faces can interfere with the main beams creating parasitic interference. Immersion cell to reduce index of refraction step as well as using of tilted MIOC faces reduce backscattering.

Optical Kerr Effect

Electric fields of the counter-propagating beams can cause changes in the index of refraction that is nonreciprocal if light is splitting at unequal parts. The nonreciprocity induced by the nonlinear Kerr effect can be strongly reduced with improving of MIOC technology.

Magneto-optical effect

The magneto-optical Faraday effect is a nonreciprocal effect which is potentially dangerous in adding to the Sagnac effect. This problem is now almost solved by the use of carefully untwisted polarization maintaining fibers as well as by using cases from special materials.

For a FOG with perfect components (ideal splitter, no backscattering, etc.), the measurement limit is imposed by the shot noise in the light as measured by photodetector. The uncertainty $\delta\Omega_\pi$, generated by the fluctuation in the light due to shot noise can be expressed as [5]:

$$\delta\Omega_\pi = \frac{c}{L \cdot D} \frac{\lambda/2}{\left(n_p n_D \tau\right)^{\frac{1}{2}}}$$

where n_p is the number of photons per second coming to photodetector, n_D is detector quantum efficiency and τ is averaging time.

The Allan variances for FOG VOBIS are shown on Fig.5-7.

V. ENVIRONMENTAL PARAMETERS

Device VOBIS successfully passed the following tests:
–low-frequency interference resistance;
–high-frequency interference resistance;
–resistance to impulse noises;
–susceptibility to electric field;
–susceptibility to constant magnetic field;
–operability tests in the conditions of vacuum with the varying mounting platform temperature in range -40°C to +50 °C;
–operability tests after the pressure reduction from normal to vacuum within the time 100s;
–accelerated life tests (140000 h) and tests on persistence (20 years);
–tests on the optical channel resistance to the impact of ionizing radiation with the total cumulative dose of radiation up to 1100 kRad.
–tests on optical elements (MIOC, fiber-optic loop, PD, SLD) resistance to the displacement damage effects when exposed to high-energy protons with fluency $2 \cdot 10^{12}$ proton/cm^2;
– test on random vibration in range 20-2000 Hz;
– test on shock with peak accelerations up to 300 g;
– test on vehicles.
The operation time of VOBIS was estimated 15 years.

VI. Flight Tests

On 28th September 2014 there was performed a successful launch of Russian GEO telecommunication satellite "Luch" (Luch means Beam (Ray)) with installed two space-grade fiber-optic gyroscopes VOBIS-1 and VOBIS-2.

Initial orientation modes of the spacecraft using VOBIS devices were correctly performed, the main and reserved VOBIS devices during checks operated correctly. No functioning not performance anomaly was detected up to now. The performances of both gyroscopes VOBIS-1 and VOBIS-2 are very close, so we give results for VOBIS-1 only.

Fig.5 shows Allan variance for VOBIS-1 obtained during acceptance test at laboratory.
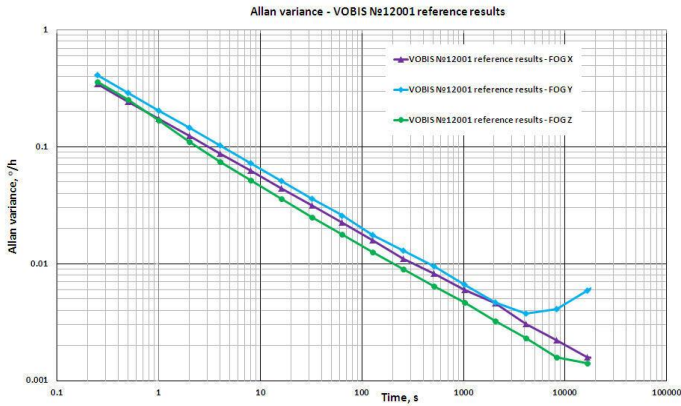

Fig. 5. Allan variance for VOBIS obtained during acceptance test at laboratory.

Fig.6 shows Allan variance for VOBIS-1 obtained during 24 hours run in December 2015 after a 15-months flight. The sampling rate was 4 Hz. For channels X and Y one can see the periodic oscillations with period around 3 seconds which corresponds to oscillations of solar panels.
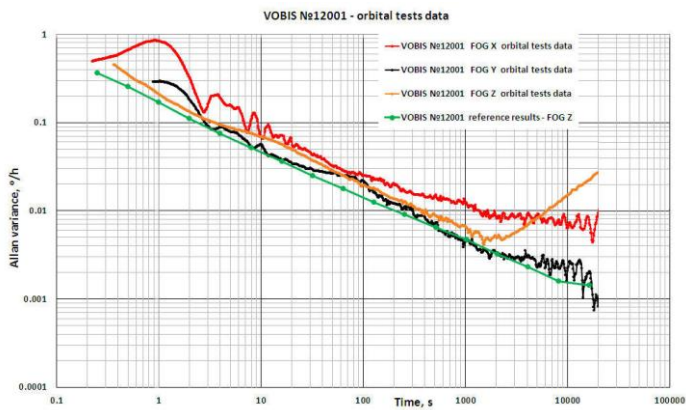

Fig. 6. Allan variance for VOBIS obtained during flight test after 15-months flight in GEO.
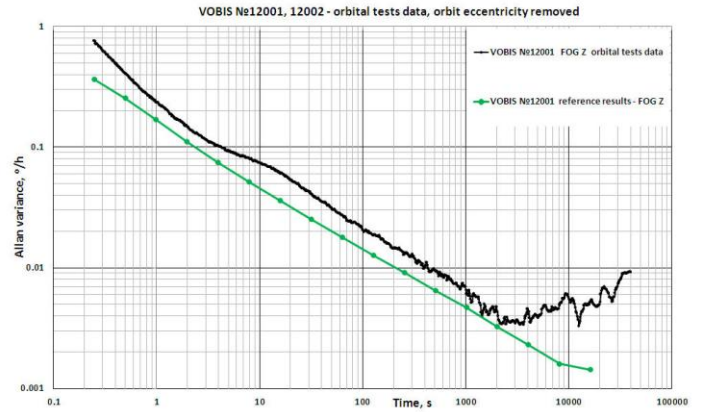

Fig. 7. Allan variance for Z-axis of VOBIS after filtering the eccentricity.

SLD current is notable increasing with fiber transmissivity degradation due to ionizing radiation. Measurement of SLD current after 15-months in GEO shown no identifiable current increase with respect to the values measured during unit manufacturing. This clearly demonstrated high radiation hardness of VOBIS units.

VII. Conclusion

Interferometric Fiber Optics Gyroscopes are ideal candidates as robust, all solid state, high reliability inertial sensors. New FOG VOBIS has been developed for space application. The gyro is tolerant to high radiation and vacuum. Extensive tests verified the gyro performance and demonstrated low noise characteristics (ARW<0.005 deg/√hr).

The gyros demonstrated in run bias stability better than 0.03 deg/hr. Performed tests shown no degradation of VOBIS accuracy parameters after 15-months flight in GEO. Such performance makes this gyro suitable for many defense and space application. Further variations of the gyro are being considered to meet specific customer demands.

References

[1] Lefevre H., The Fiber-Optic Gyroscope, Artech House, 1993.

[2] Y.N.Korkishko, V.A.Fedorov, and O.Y. Feoktistova, "LiNbO$_3$ optical waveguide fabrication by high-temperature proton-exchange", IEEE J. Lightwave Technol., vol.18, pp.562-568, 2000.

[3] P.G.Suchoski, T.K.Findakly, and F.J. Leonberger, "Stable low-loss proton-exchanged LiNbO$_3$ devices with no electro-optic degradation", Opt. Lett., vol.13, pp.1050-1052, 1988.

[4] Y.N.Korkishko and V.A.Fedorov, "Structural Phase Diagram of HxLi1-xNbO$_3$ waveguides: The Correlation Between Structural and Optical Properties", IEEE Journal of Selected Topics in Quantum Electronics, vol.2, pp. 187-196, 1996.

[5] J.L. Davis, and S. Ezekiel, "Techniques for shot noise limited inertial rotation measurement using a multiturn fiber Sagnac interferometer", Proc.SPIE, vol.157, pp.131-137, 1978.